

## Phase time for a tunneling particle

Swarnali Bandopadhyay

*Department of Physics, Ben-Gurion University, Beer-Sheva 84105, Israel*  
*swarnali@bgu.ac.il*

A. M. Jayannavar

*Institute of Physics, Sachivalaya Marg, Bhubaneswar 751005, India*  
*jayan@iopb.res.in*

We study the nature of tunneling phase time for various quantum mechanical structures such as networks and rings having potential barriers in their arms. We find the generic presence of Hartman effect, with superluminal velocities as a consequence, in these systems. In quantum networks it is possible to control the ‘super arrival’ time in one of the arms by changing the parameters on another arm which is spatially separated from it. This is yet another quantum nonlocal effect. Negative time delays (time advancement) and ‘ultra Hartman effect’ with negative saturation times have been observed in some parameter regimes. In presence and absence of Aharonov-Bohm (AB) flux quantum rings show Hartman effect. We obtain the analytical expression for the saturated phase time. In the opaque barrier regime this is independent of even the AB flux thereby generalizing the Hartman effect. We also briefly discuss the concept of “space collapse or space destroyer” by introducing a free space in between two barriers covering the ring. Further we show in presence of absorption the reflection phase time exhibits Hartman effect in contrast to the transmission phase time.

*Keywords:* Tunneling, Electronic transport  
*PACS numbers:* 03.65.-w; 73.40.Gk; 84.40.Az; 03.65.Nk; 73.23.-b

### 1. Introduction

Quantum tunneling, where a particle has finite probability to penetrate a classically forbidden region is an important feature of wave mechanics. Invention of the tunnel diode<sup>1</sup>, the scanning tunneling microscope<sup>2</sup> etc. made the quantum tunneling useful from a technological point of view. In 1932 MacColl<sup>3</sup> pointed out that tunneling is not only characterized by a tunneling probability but also by a time the tunneling particle takes to traverse the barrier. There has been considerable interest on the question of time spent by a particle in a given region of space<sup>4,5,6</sup>. The recent developments of nanotechnology brought new urgency to study the tunneling time as it is directly related to the maximum attainable speed of nanoscale electronic devices. In addition, recent experimental results claiming superluminal tunneling speeds for photons<sup>7,8</sup> call for detailed analysis of this problem. In a number of numerical<sup>9</sup>, experimental<sup>7,10</sup> and analytical study of quantum tunneling processes, various def-

2 *Swarnali Bandopadhyay, A. M. Jayannavar*

initions of tunneling times have been investigated. These different time scales are based on various different operational definitions and physical interpretations. Till date there is no clear consensus about the existence of a simple expression for this time as there is no hermitian operator associated with it<sup>4</sup>. Furthermore, a corpuscular picture of tunneling is very hard to be realized due to the lack of a direct classical limit for the trajectories and velocities of the tunneling particle.

Among the various time scales, ‘*dwell time*’<sup>11</sup> which gives the duration of a particle’s stay in the barrier region regardless of how it escapes can be calculated as the total probability of the particle inside the barrier divided by the incident probability current. The ‘*conditional sojourn time*’<sup>6</sup> gives the time of sojourn (dwell) in the spatial region of interest for some given conditions of scattering. It can be defined meaningfully by a ‘clock’ which is basically an extra degree of freedom that co-evolves with the sojourning particle. Büttiker and Landauer proposed<sup>12</sup> that one should study ‘tunneling time’ using the transmission coefficient through a static barrier of interest, supplemented by a small oscillatory perturbation. This is referred to as ‘*Büttiker-Landauer time*’ in the literature. In another approach, the traversal time, is measured by the spin precession of the tunneling particle in a uniform infinitesimal magnetic field. This is called local ‘*Larmor time*’<sup>11,13</sup>. A large number of researchers interpret the ‘*phase time*’<sup>5,14,15</sup> as the temporal delay of a transmitted wave packet. This time is usually taken as the difference between the time at which the peak of the transmitted packet leaves the barrier and the time at which the peak of the incident quasi-monochromatic wave packet arrives at the barrier. Within the stationary phase approximation, the phase time can be calculated from the energy derivative of the ‘phase shift’ in the transmitted or reflected amplitudes. It would be worth mentioning that for a symmetric barrier, the reflection and transmission phase times are equal. For tunneling through a 1D static barrier due to the time-reversal symmetry, one can show from the unitarity of the scattering matrix that the phases of the reflection and transmission amplitudes differ by a constant, quantitatively by  $\pi/2$ . However this does not remain true for asymmetric/complex barrier. Büttiker-Landauer<sup>12</sup> raised objection that the peak is not a reliable characteristic of packets as the wave packet may undergo strong distortion or deformation after tunneling through the barrier. Moreover, there is no causal relationship between the peak of the transmitted wave packet and the peak of the incident packet. This is due to the fact that the peak of the transmitted packet can leave the scattering region before the peak of the incident packet has arrived. In contrast to ‘dwell time’ which can be defined locally, the ‘phase time’ is essentially asymptotic in character<sup>16</sup>. The ‘phase time’ statistics is intimately connected with dynamic admittance of micro-structures<sup>17</sup>. The ‘phase time’ is also directly related to the density of states<sup>18,19,20,21</sup>. The universality of ‘phase time’ distributions in random and chaotic systems has already been established earlier<sup>22</sup>. In the case of ‘not too opaque’ barriers, the tunneling time evaluated either as a simple ‘phase time’<sup>5</sup> or calculated through the analysis of the wave packet behaviour<sup>23</sup> becomes independent of the barrier width. This phenomenon is termed as the Hartman

effect<sup>15,23,24</sup>. This implies that for sufficiently long barriers the effective velocity of the particle can become arbitrarily large, even larger than the light speed in the vacuum (superluminal effect). Though this interpretation is a little far fetched for non-relativistic Schrödinger equation as velocity of light plays no role in it, this effect has been established even in relativistic quantum mechanics.

Tunneling time associated with electron being very small ( $\sim$  femto second) the experiments to verify the ‘Hartman effect’ (generalized Hartman effect) are usually done on optical waveguide where the corresponding time is of the order of pico second. However the formal analogy between the Schrödinger equation and the Helmholtz equation for electromagnetic wave enables one to correlate the results for optical experiments to that for electrons. Photonic experiments show that electromagnetic pulses travel with group velocities in excess of the speed of light in vacuum as they tunnel through a constriction in a waveguide<sup>8</sup>. Experiments with photonic band-gap structures clearly demonstrate that ‘tunneling photons’ indeed travel with superluminal group velocities<sup>7</sup>. Their measured tunneling time is practically obtained by comparing the two peaks of the incident and transmitted wave packets. Thus all these experiments directly or indirectly confirmed the occurrence of Hartman effect without violating ‘Einstein causality’ *i.e.*, the signal velocity or the information transfer velocity is always bounded by the velocity of light. It should also be noted that in the photonic tunneling time experiments by Nimtz *et. al.*, based on frustrated total internal reflection, the velocity of the half-width of the pulse (not the peak of the wave packet) is monitored. The velocity of the half-width is found to be superluminal (according to theory and experiment). Relation of this result to the causality principle is discussed in the references<sup>25,26</sup>. The ‘Hartman effect’ has been extensively studied both for nonrelativistic (Schrödinger equation) and relativistic (Dirac equation)<sup>4,5,8</sup> cases. Recently Winful<sup>27</sup> showed that the saturation of phase time is a direct consequence of saturation of integrated probability density under the barrier (equivalently in the electromagnetic waves saturation of stored energy). The Hartman effect has been found in one dimensional barrier tunneling<sup>23</sup> as well as in tunneling through mesoscopic rings in presence of Aharonov-Bohm (AB) flux<sup>28</sup>. In the present work we extend the study of phase times for branched quantum networks and rings.

The main results of this paper are as follows:

- We have found Hartman effect in barrier tunneling regime for quantum networks and rings.
- In quantum networks non-locality and time-advancement (negative time delay) are found.
- In presence of AB-flux in the rings saturated phase time becomes independent of the flux. Thus the Hartman effect is obtained even in presence of AB-flux.
- We obtain space collapse in quantum ring *i.e.* in presence of inter-barrier free space the phase time becomes independent of the length of this free

4 *Swarnali Bandopadhyay, A. M. Jayannavar*

space in the off resonance regimes.

- Even in presence of absorption in the barrier, the reflection phase time shows Hartman effect though the transmission phase time grows with the length of the barrier.

The paper is organized as follows. In section 2 we present phase times<sup>29</sup> for branched networks of quantum wires which can readily be realized in optical wave propagation experiments. This geometry allows us to check other nonlocality effect such as tuning of the saturation value of ‘phase time’ and consequently the superluminal speed in one branch by changing barrier strength or length in any other branch, spatially separated from the former. In section 3 we study the Hartman effect on a quantum ring geometry *i.e.* beyond one dimension and in the presence of AB-flux<sup>28,30</sup>. Our results confirm ‘Hartman effect’ in quantum ring even in presence of AB-flux. Then we study the phase time in quantum ring in absence of AB-flux. In tunneling through the ring having two potential barriers with an intermediate free space where a quantum particle can propagate as a traveling wave, the saturated phase time becomes independent of the intermediate free length (in the large length limit of the barriers) in the off resonant cases. This result can be interpreted as a “space collapse or space destroyer”<sup>31</sup>, as if the intermediate free space does not exist. We also show that in the presence of absorption in barrier regime the Hartman effect survives in the reflection mode as opposed to the transmission mode. Then in section 4 we summarize our results and conclude.

## 2. Hartman effect and non-locality in quantum networks

Hartman effect is itself one of the manifestations of quantum non-locality<sup>7</sup>. Here we study the effect for various quantum mechanical networks having potential barriers in their arms. In such systems it is possible to control the ‘super arrival’ time in one of the arms by changing parameters on another, spatially separated from it. This is yet another quantum nonlocal effect. Negative time delays (time advancement) and ‘ultra Hartman effect’ with negative saturation times have been observed in some parameter regimes.

As a model system we choose a network of wires. The length of these wires are so narrow that only the motion along the length of the wires is of interest (a single channel case). The motion in the perpendicular direction is frozen in the lowest transverse sub-band. In a three-port Y-branch circuit (Fig. 1) the two side branches of quantum wire  $S_1$  and  $S_2$  are connected to a ‘base’ arm  $S_0$  at the junction  $J$ . In general one can have  $N(\geq 2)$  such side branches connected to the ‘base’ wire.

We study the scattering problem across a network geometry as presented schematically in Fig. 1. Such geometries are important from the point of view of basic science due to their properties of tunneling and interference<sup>32,33</sup> as well as of technological applications such as wiring in nano-structures. In particular, the Y-junction carbon nanotubes are in extensive studies and they show various interesting properties like asymmetric current voltage characteristics<sup>34</sup>. In our system of

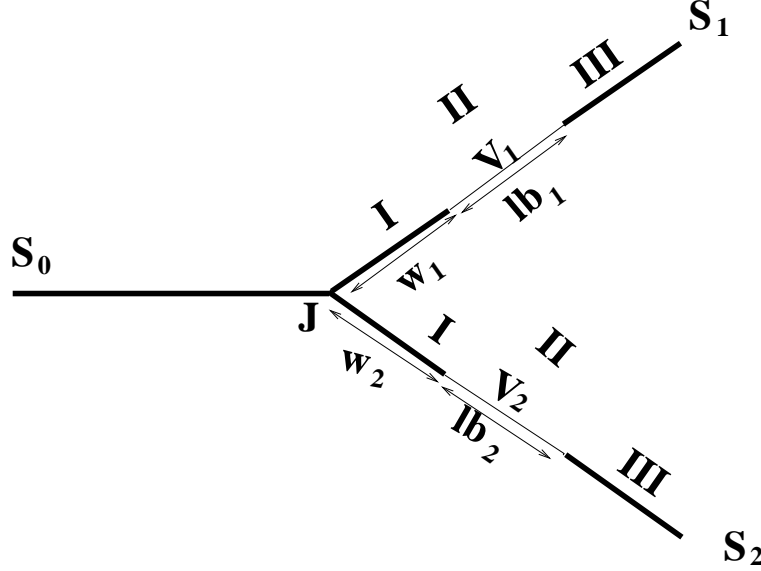


Fig. 1. Schematic diagram of a Y-junction or three-way splitter.

interest there are finite quantum mechanical potential barriers of strength  $V_1$  and  $V_2$  and length  $lb_1$  and  $lb_2$  in the side branches  $S_1$  and  $S_2$  respectively. We focus on a situation wherein the incident electrons have an energy  $E$  less than  $V_n$ ,  $n = 1, 2$ . The impinging electrons in this sub-barrier regime travel as an evanescent mode/wave and the transmission involve contributions from quantum tunneling and multiple reflections between each pair of barriers and the junction point. Here we are interested in a single channel case where the Fermi energy lie in the lowest sub-band. To excite the evanescent modes in the side branches one has to produce constrictions by making the length of the regions of wires containing barriers much thinner than that of the other parts of the wire. The electrons occupying the lowest sub-band in the connecting wire on entering the constrictions experience a potential barrier (due to higher quantum zero point energy) and propagate as an evanescent mode<sup>35,36</sup>. In this work an analysis of the phase time or the group delay time in such a system is carried out.

### 2.1. Theoretical treatment

We approach this scattering problem using the quantum wave guide theory<sup>37,38</sup>. In the stationary case the incoming particles are represented by a plane wave  $e^{ikx}$  of unit amplitude. The effective mass of the propagating particle is  $m$  and the energy is  $E = \hbar^2 k^2 / 2m$  where  $k$  is the wave vector corresponding to the free particle. The wave functions, in different regions of the system considered in Fig. 1 can be written

6 *Swarnali Bandopadhyay, A. M. Jayannavar*

as,

$$\begin{aligned}
 \psi_{in}(x_0) &= e^{ikx_0} + R e^{-ikx_0} \quad (\text{in } S_0), \\
 \psi_{(1)I}(x_1) &= A_1 e^{ikx_1} + B_1 e^{-ikx_1} \quad (\text{region I in } S_1), \\
 \psi_{(2)I}(x_2) &= A_2 e^{ikx_2} + B_2 e^{-ikx_2} \quad (\text{region I in } S_2), \\
 \psi_{(1)II}(x_1) &= C_1 e^{-\kappa_1(x_1-w_1)} + D_1 e^{\kappa_1(x_1-w_1)} \quad (\text{region II in } S_1), \\
 \psi_{(2)II}(x_2) &= C_2 e^{-\kappa_2(x_2-w_2)} + D_2 e^{\kappa_2(x_2-w_2)} \quad (\text{region II in } S_2), \\
 \psi_{(1)III}(x_1) &= t_1 e^{ik(x_1-w_1-lb_1)} \quad (\text{region III in } S_1), \\
 \psi_{(2)III}(x_2) &= t_2 e^{ik(x_2-w_2-lb_2)} \quad (\text{region III in } S_2),
 \end{aligned}$$

with  $\kappa_n = \sqrt{2m(V_n - E)/\hbar^2}$  being the imaginary wave vector in presence of a rectangular barrier of strength  $V_n$ , with  $n = 1, 2$ .  $x_0$  is the spatial coordinate for the ‘base’ wire, whereas  $x_1$  and  $x_2$  are the spatial coordinates for the  $S_1$  and  $S_2$  side branches respectively. All these coordinates are measured from the junction  $J$ .  $w_1$  and  $w_2$  are the distances between the junction  $J$  and the respective barriers in arm  $S_1$  and  $S_2$ .

To solve the problem, we use Griffith’s boundary conditions<sup>39</sup>

$$\psi_{in}(x_0 = J) = \psi_{(1)I}(x_1 = J) = \psi_{(2)I}(x_2 = J), \quad (1)$$

and

$$\left. \frac{\partial \psi_{in}(x_0)}{\partial x_0} \right|_J = \left. \frac{\partial \psi_{(1)I}}{\partial x_1} \right|_J + \left. \frac{\partial \psi_{(2)I}}{\partial x_2} \right|_J, \quad (2)$$

at the junction  $J$ . All the derivatives are taken either outward or inward from the junction<sup>37</sup>. In each side branch, at the starting and end points of the barrier, the boundary conditions can be written as

$$\psi_{(n)I}(x_n = w_n) = \psi_{(n)II}(x_n = w_n), \quad (3)$$

$$\psi_{(n)II}(x_n = w_n + lb_n) = \psi_{(n)III}(x_n = w_n + lb_n), \quad (4)$$

$$\left. \frac{\partial \psi_{(n)I}}{\partial x_n} \right|_{(w_n)} = \left. \frac{\partial \psi_{(n)II}}{\partial x_n} \right|_{(w_n)}, \quad (5)$$

$$\left. \frac{\partial \psi_{(n)II}}{\partial x_n} \right|_{(w_n+lb_n)} = \left. \frac{\partial \psi_{(n)III}}{\partial x_n} \right|_{(w_n+lb_n)}, \quad (6)$$

where  $n = 1, 2$ . From the above mentioned boundary conditions one can obtain the complex transmission amplitudes  $t_1$  and  $t_2$  on the side branches  $S_1$  and  $S_2$  respectively.

## 2.2. Results and Discussions

Following the method introduced by Wigner<sup>14</sup>, we can calculate the ‘phase time’ (phase time for transmission) from the energy derivative of the phase of the transmission amplitude  $t_n$ <sup>5,14</sup> as

$$\tau_n = \hbar \frac{\partial \text{Arg}[t_n]}{\partial E}. \quad (7)$$

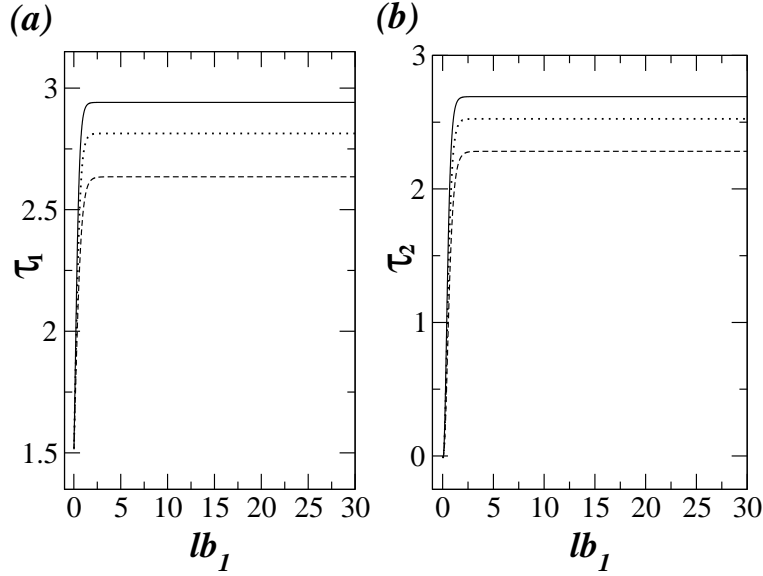


Fig. 2. For a 3-way splitter with a barrier in  $S_1$  arm, the ‘phase times’  $\tau_1$  and  $\tau_2$  are plotted as a function of barrier length ‘ $lb_1$ ’ in (a) and (b) respectively. The solid, dotted, dashed curves are for  $V_1 = 5, 4, 3$  respectively. Other system parameters are  $E = 1, w_1 = 3$ .

In what follows, we set  $\hbar = 1$  and  $2m = 1$ . We now proceed to analyze the behavior of  $\tau_n$  as a function of various physical parameters for different network topologies. We measure time at the far end of each barrier in the branched arms containing barriers and in the case of arms in absence of any barrier we measure the phase time at the junction points. We express all the physical quantities in dimensionless units *i.e.* all the barrier strengths  $V_n$  in units of incident energy  $E$  ( $V_n \equiv V_n/E$ ), all the barrier lengths  $lb_n$  in units of inverse wave vector  $k^{-1}$  ( $lb_n \equiv k lb_n$ ), where  $k = \sqrt{E}$  and all the extrapolated phase time  $\tau_n$  in units of inverse of incident energy  $E$  ( $\tau_n \equiv E\tau_n$ ).

First we take up a system similar to the Y-junction shown in Fig. 1 in presence of a barrier  $V_1$  of length  $lb_1$  in arm  $S_1$  but in absence of any barrier in arm  $S_2$ . For a tunneling particle having energy  $E < V_1$  we find out the phase time  $\tau_1$  in arm  $S_1$  as well as  $\tau_2$  in arm  $S_2$  as a function of barrier length  $lb_1$  (Fig. 2). From Fig. 2(a) it is clear that  $\tau_1$  evolves with  $lb_1$  and eventually saturates to  $\tau_{1s}$  for large  $lb_1$  to show the Hartman effect. Fig. 2(b) shows the phase time  $\tau_2$  in arm  $S_2$  which does not contain any barrier. This also evolves and saturates with  $lb_1$ , the length of the barrier in the other arm  $S_1$ . This delay is due to the contribution from paths which undergo multiple reflection in the first branch before entering the second branch via junction point  $J$ . In absence of a barrier in the  $n$ -th arm the phase time  $\tau_n$  measured close to the junction  $J$  should go to zero *i.e.*  $\tau_n \rightarrow 0$  in the absence of multiple scatterings in the first arm. Note that  $\tau_{1s}$  and  $\tau_{2s}$  change with energies of

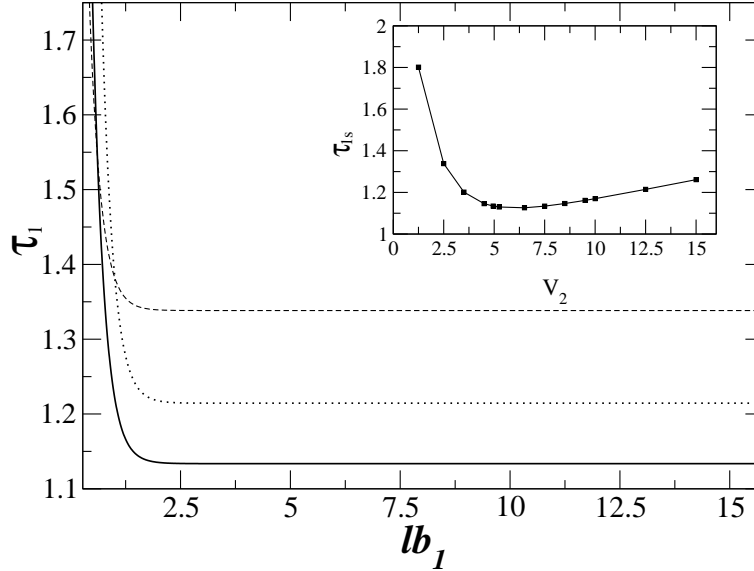
8  $S_w$ 


Fig. 3. Here for a 3-way splitter with one barrier in each branched arm  $S_1$  and  $S_2$ , the ‘phase time’  $\tau_1$  is plotted as a function of barrier length ‘ $lb_1$ ’ keeping  $lb_2(=1)$  and  $V_1(=5)$  fixed and for different values of parameter  $V_2$ . The dashed, solid and dotted curves are for  $V_2 = 2.5, 5.0$  and  $12.5$  respectively. Other system parameters are  $E = 1, w_1 = w_2 = 3$ . In the inset  $\tau_{1s}$  is plotted as a function of  $V_2$  for the same system parameters.

the incident particle (Fig. 2). From Fig.2 it can be easily seen that  $\tau_{2s}$  is always smaller than  $\tau_{1s}$  for any particular  $V_1$  *i.e.* the saturation time in the arm having no barrier is smaller. The phase time in both the arms show non-monotonic behavior as a function of  $V_1$ . As we decrease the strength of the barrier  $V_1$  the value of  $\tau_1$  ( $\tau_2$ ) decreases in the whole range of lengths of the barrier and also the saturated value of  $\tau_{1s}$  ( $\tau_{2s}$ ) decreases until  $V_1$  reaches 1.6 and with further decrease in  $V_1$  the values of  $\tau_1$  ( $\tau_2$ ) as well as  $\tau_{1s}$  ( $\tau_{2s}$ ) starts increasing.

As the second case we take up another Y-junction which contain potential barriers in both of its side branches as shown in Fig. 1. We fix the values of  $V_1(=5)$  and vary  $lb_1$  for each values of  $V_2$  to study the  $lb_1$ -dependence of  $\tau_1$  (Fig.3). From Fig. 3 we see that  $\tau_1$  decreases with increase in  $lb_1$  and saturate to a value  $\tau_{1s}$  at each value of  $V_2$  thereby showing ‘Hartman effect’ for arm ‘ $S_1$ ’. But now, we can tune the saturation phase time *i.e.* speed of the peak of the wave packet in one arm  $S_1$  non-locally by tuning the strength of the barrier potential  $V_2$  sitting on the other arm  $S_2$ ! Thus ‘quantum nonlocality’ enables us to control the ‘super arrival’ time in one of the arms ( $S_1$ ) by changing a parameter ( $V_2$ ) on the other, spatially separated from it. In the inset of Fig. 3 we plot  $\tau_{1s}$  as a function of  $V_2$ . It clearly shows that when the barrier strengths  $V_1$  and  $V_2$  are very close the ‘phase time’ reaches its minimum value. In all other cases *i.e.*, whenever  $V_1 \neq V_2$ , the value of  $\tau_{1s}$  is larger.



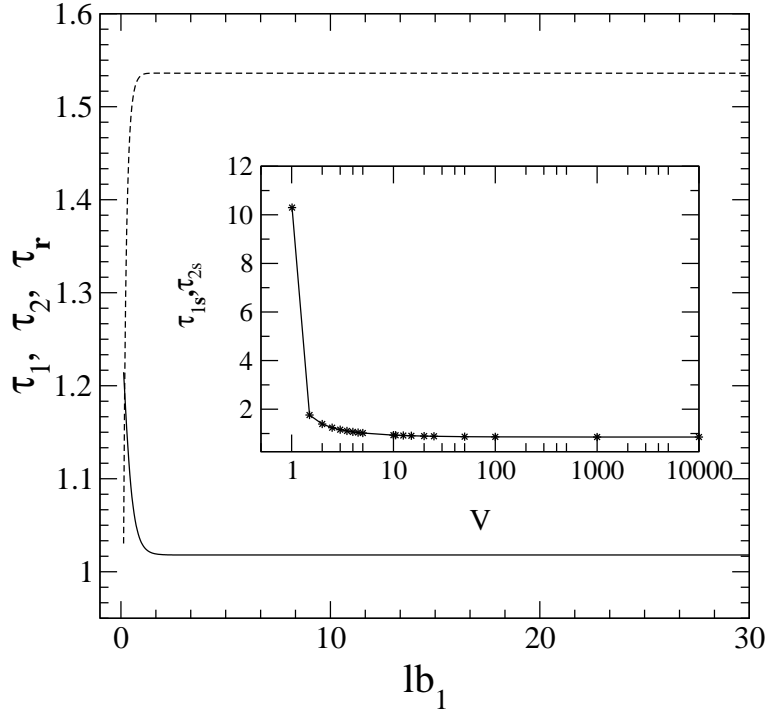


Fig. 4. Here for a 3-way splitter with an identical barrier in each branched arm  $S_1$  and  $S_2$ , the ‘phase times’ are plotted as a function of barrier length ‘ $lb_1$ ’ ( $= lb_2$ ) for fixed  $V_1 = V_2 (= 5)$ . The solid and dashed curves represent  $\tau_1$  ( $= \tau_2$ ) and  $\tau_r$  respectively. Other system parameters are  $E = 1, w_1 = w_2 = 2.5$ . In the inset  $\tau_{1s}$  ( $= \tau_{2s}$ ) is plotted as a function of  $V$  ( $= V_1 = V_2$ ) for the same system parameters.

With the above system but for two identically branched arms (i.e.,  $V_1 = V_2$ ,  $w_1 = w_2$  and  $lb_1 = lb_2$ ) we study the behaviour of different phase times as a function of  $lb_1$ . For this case we see from Fig. 4 that  $\tau_1$  and  $\tau_2$  are the same, as expected. The phase time in reflection mode, measured near the junction on base arm, evolves differently from these two phase times. The reflection phase time getting saturated with increasing barrier’s length confirms Hartman effect. The value of saturated reflection phase time is also different from that of the transmission mode. We also study the saturated transmission phase times by changing the strength of the barriers. From the inset of Fig. 4, we see that for strength very close to the value of the incident energy the saturated phase time is quite large and the saturated phase time decreases with the increasing barrier strength.

We shall now show another interesting result related to the Hartman effect. For this we keep  $V_2 (= 5)$  unaltered and reduce  $lb_2$ . For very small  $lb_2 (= 0.5)$  we see from Fig. 5 that  $\tau_1$  is negative for almost the whole range of  $lb_1$ -values showing ‘time-advancement’ and eventually after a sharp decrease saturates to a negative value of  $\tau_{1s} = -4.514$  implying ‘Hartman effect’ with advanced time or ‘ultra Hartman

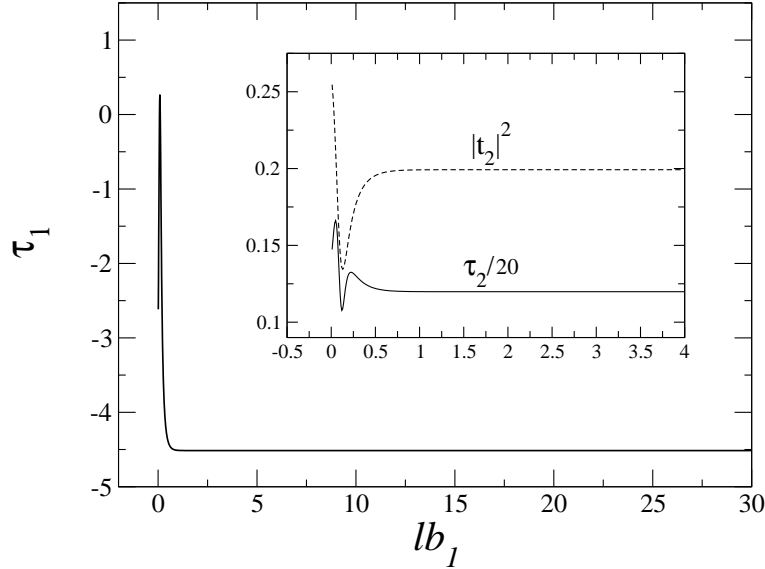


Fig. 5. Here for a 3-way splitter with one barrier in each side branch  $S_1$  and  $S_2$ , the ‘phase time’  $\tau_1$  is plotted as a function of ‘ $lb_1$ ’ for a very small  $lb_2 (= 0.5)$ . Other system parameters are  $E = 1$ ,  $w_1 = w_2 = 2.5$ ,  $V_2 = 5$  and  $V_1 = 15$ . In the inset, the solid and dashed curves represent  $\tau_2$  and  $|t_2|^2$  respectively as a function of  $lb_1$ . For better visibility we have plotted phase times scaled down by a factor of 20.

effect’. In the inset we plot the corresponding  $\tau_2$  and  $|t_2|^2$  as a function of  $lb_1$ . The tunneling phase time for an one dimensional barrier with the same strength  $V_2$  and width  $lb_2$ , as used in the side branch  $S_2$  of the network, is different from  $\tau_2$ , obtained for the whole range of values of  $lb_1$ . This is due to the presence of the other arm in the network problem. In the cases discussed so far  $\tau_2$  vary more sharply in small  $lb_1$  regime. Furthermore, the inset in Fig. 5 shows a dip in  $\tau_2$  at parameter regimes where  $|t_2|^2$  has a minimum.

For a wave packet with large spread in real space it is possible that the leading edge of the wave packet reaches the barrier much earlier than the peak of the packet. This leading edge in turn can tunnel through the barrier to produce a peak in the other end much before the peak of the incident wave packet reaches the barrier region. This sometimes is referred to as pulse reshaping effect. This, in general, causes ‘time advancement’<sup>4</sup>. This negative delay does not violate causality, however, this delay time is bounded from below. In 1D barrier such a situation does not arise. In presence of square wells in one dimensional systems negative time delays have been observed. This effect is termed as ‘ultra Hartman effect’ [ see for details<sup>40</sup> ].

As the next case we set the length of the barrier in arm  $S1$  of the above mentioned system at a large value (say 100) where all the phase times get saturated. Now we shift the position of the barrier in arm  $S2$  away from the junction and study its effect on the saturated transmission and reflection phase times. In Fig. 6 we have

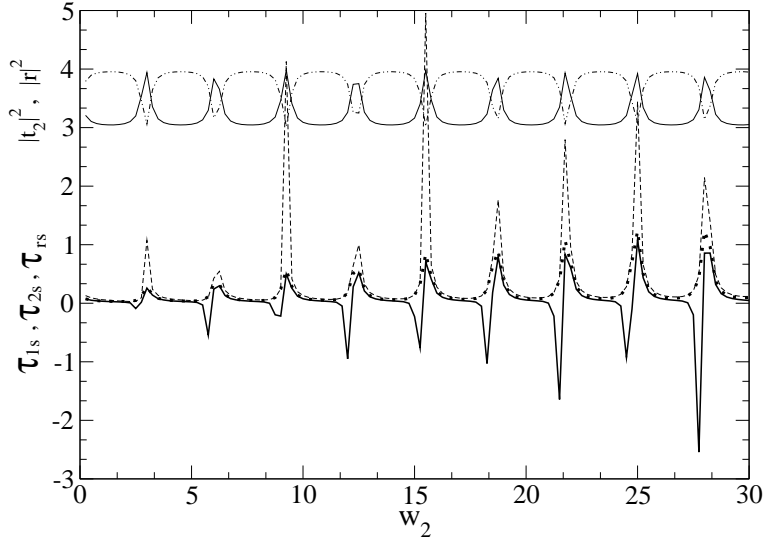


Fig. 6. For a 3-way splitter with one barrier in each side branch  $S_1$  and  $S_2$ ,  $\tau_{1s}/50$  (thick solid),  $\tau_{2s}/50$  (thick dotted) and  $\tau_{rs}/50$  (dashed) are shown as a function of ' $w_2$ '.  $|t_2|^2$  (solid) and  $|r|^2$  (double dot-dashed) are shifted upwards along the the positive  $y$ -direction by 3. The different system parameters are  $E = 1$ ,  $V_1 = 15$ ,  $V_2 = 5$ ,  $lb_1 = 100.0$ ,  $lb_2 = 0.5$  and  $w_1 = 2.5$ .

plotted all these three quantities  $\tau_{1s}$ ,  $\tau_{2s}$  and  $\tau_{rs}$  as a function  $w_2$ . Earlier we had shown in Fig. 3 that by changing a nonlocal parameter  $V_2$  one can tune  $\tau_{1s}$  whereas Fig. 6 shows that change of another parameter  $w_2$  can tune  $\tau_{1s}$  nonlocally. Note that  $\tau_{2s}$  and  $\tau_{rs}$  also depend on  $w_2$ . From Fig. 6 we see that  $|t_2|^2$  ( $|r|^2$ ) shows resonances (anti-resonances) as a function of  $w_2$ . The saturated delay time  $\tau_{1s}$  exhibit sharp variation in phase time around the resonance. Moreover, it takes negative as well as positive values. Around the resonance sharp peaks exist in both positive and negative side. In contrast to this observation of  $\tau_{1s}$  the other two phase times show only positive peaks. As  $|t_2|^2$  and  $|r|^2$  have finite non-zero values, these variations in phase times should, in principle, be observable in experiments. In Fig. 7 we have plotted  $\tau_{1s}$  as a function of  $w_2$  for two different values of the length  $lb_2$  of the barrier in arm  $S_2$ . Note that as we increase the length  $lb_2$ , the frequency of getting negative saturation values ( $\tau_{1s}$ ) reduces (see the solid curve in Fig. 7) and increasing the length  $lb_2$  further, the negative saturation goes away. This is in agreement with the discussions in previous paragraph. The saturation to a negative value can be attributed to the nonidentical barriers in two branched arms, the barrier length of one being very small compared to the other. When  $lb_1 = lb_2$  the time-advancement goes away.

So far our discussion is based on wave guide theory of transport. We can as well treat the junction as a scatterer described by the following one parameter scattering

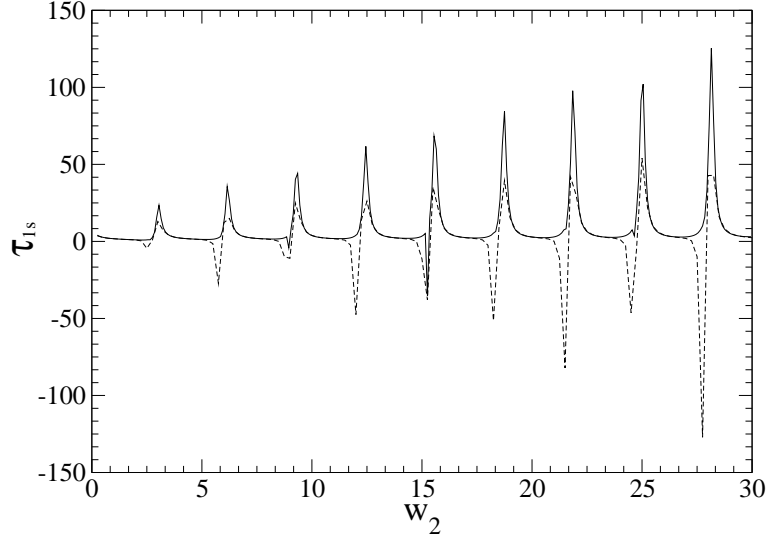
12 *Swa*


Fig. 7. Here for a 3-way splitter with one barrier in each side branch  $S_1$  and  $S_2$ , the ‘saturated phase time’  $\tau_{1s}$  is plotted as a function of ‘ $w_2$ ’. The dashed and solid curves are for  $lb_2 = 0.5$  and  $2.0$  respectively. Other system parameters are  $E = 1$ ,  $V_1 = 15$ ,  $V_2 = 5$ ,  $lb_1 = 100.0$  and  $w_1 = 2.5$ .

matrix<sup>41</sup>

$$S_J = \begin{pmatrix} -(a+b) & \sqrt{\epsilon} & \sqrt{\epsilon} \\ \sqrt{\epsilon} & a & b \\ \sqrt{\epsilon} & b & a \end{pmatrix} \quad (8)$$

where  $a = \frac{1}{2}(\sqrt{1-2\epsilon} - 1)$  and  $b = \frac{1}{2}(\sqrt{1-2\epsilon} + 1)$ .  $\epsilon$  is a coupling parameter with values  $0 \leq \epsilon \leq 0.5$ . When  $\epsilon \rightarrow 0$  the side branches are decoupled from the base arm while for  $\epsilon \rightarrow 0.5$  they are strongly coupled. This  $S$ -matrix satisfies the conservation of current<sup>42,43</sup>. For our network system with two side branches, the equations at the junction  $J$  can be written as

$$\begin{pmatrix} R \\ A_1 \\ A_2 \end{pmatrix} = S_J \begin{pmatrix} 1 \\ B_1 \\ B_2 \end{pmatrix}. \quad (9)$$

We have studied the effect of the coupling parameter  $\epsilon$  on the Hartman effect. From Fig. 8, we see that though the nature of  $\tau_1$  and  $\tau_2$  as a function of  $lb_1$  does not depend on the coupling parameter  $\epsilon$  but their saturation value is strongly dependent on  $\epsilon$ . For weak coupling, the value of saturated phase time is quite low and it increases with increasing strength of the coupling between base arm and side branches. For  $\epsilon = 4/9$  we get back the results obtained earlier using the wave-guide theory (compare the solid curves in Fig. 8 with the dashed curves in Fig. 2).

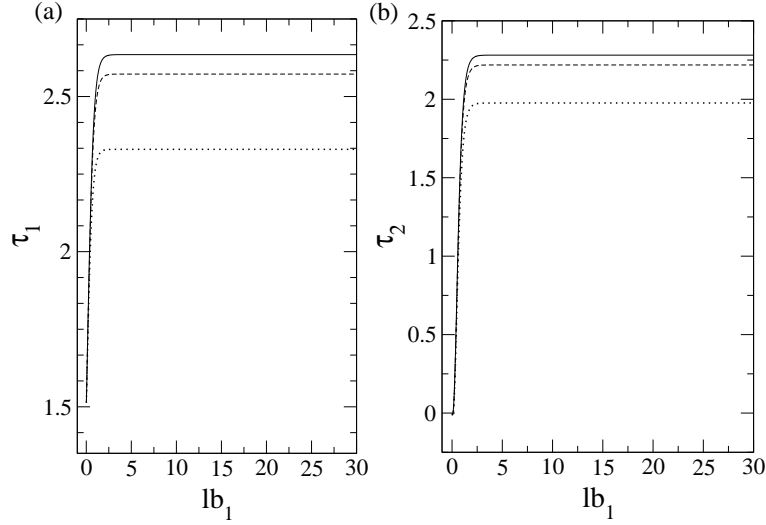


Fig. 8. For a 3-way splitter with a barrier in  $S_1$  arm, the ‘phase times’  $\tau_1$  and  $\tau_2$  are plotted as a function of barrier length ‘ $lb_1$ ’ in (a) and (b) respectively. The dotted, dashed and solid curves are for the junction coupling parameter  $\epsilon = 1/9, 1/3, 4/9$  respectively. Other system parameters are  $V_1 = 3, E = 1, w_1 = 3$ . We see that both  $\tau_{1s}$  and  $\tau_{2s}$  increase as we increase the coupling strength.

### 3. Hartman effect in Quantum ring

In this section we study the scattering problem across a quantum ring connected to one ideal semi infinite lead (as shown schematically in Fig. 9). Such ring geometry systems are extensively investigated in mesoscopic physics in analyzing normal state Aharonov-Bohm effect which has been observed experimentally<sup>32,33</sup>. A magnetic field is applied perpendicular to the plane of the ring. Due to this a magnetic flux  $\phi$  as shown in Fig. 9, enclosed by the ring, there is a finite quantum mechanical potential of strength  $V$  inside the ring while that in the connecting lead is set to be zero. We focus on a situation wherein the incident electrons have an energy  $E$  less than  $V$ . The impinging electrons in this sub-barrier regime travels as an evanescent mode throughout the circumference of the ring and the reflection or the conductance involve contributions from both the Aharonov-Bohm effect as well as quantum tunneling. Here we are interested in a single channel case where the Fermi energy lies in the lowest sub-band. To excite the evanescent modes in the ring we have to make the width of the ring much less than that of the connecting lead. The electrons occupying the lowest sub-band in the lead on entering the ring experience a higher barrier (due to higher quantum zero point energy) and propagate in the ring as evanescent mode. The transmission or conductance across such systems has been studied in detail<sup>35,36</sup>. An analysis of the phase time for such a ring system is carried out in the following subsections.

Now we discuss the ‘reflection phase time’ for the above quantum ring in pres-

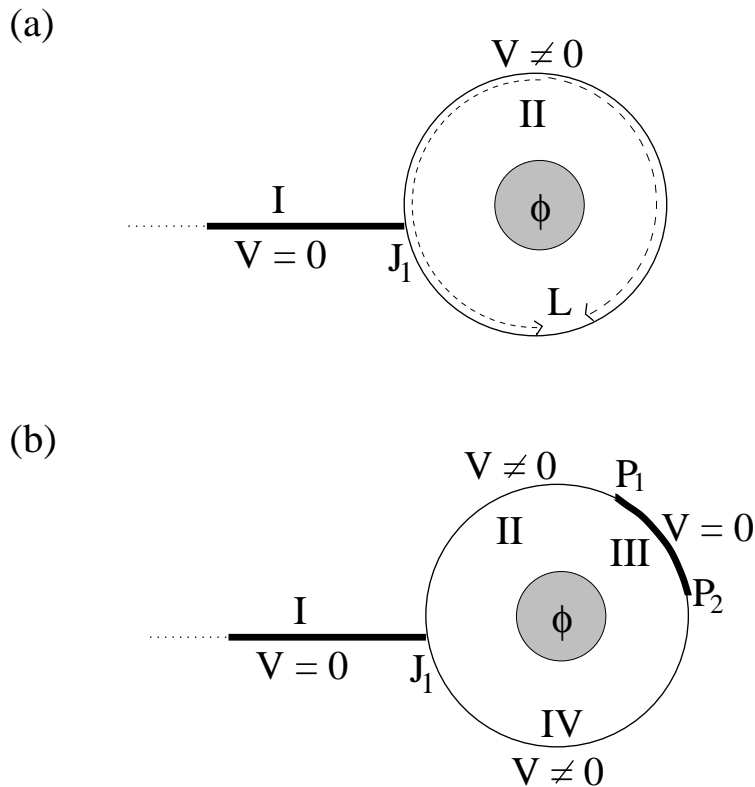


Fig. 9. Schematic diagram of a circular ring connected to semi infinite lead.

ence of AB-flux as shown in Fig 9(a). It is well known that in one dimensional scattering/tunneling problem, reflection involves prompt part as well as the multiple scattering arising from the edges of the scattering center (say, for the square barrier). However, transmission across the scattering region does not have the prompt part but has only contributions from multiple scattering. We would like to emphasize here the fact that the unitarity of the scattering matrix forces transmission and reflection phase times to coincide for a one dimensional tunneling problem (to be identical in magnitude), even though reflection has a prompt part as mentioned above. Hence, the information we get does not depend on whether we study the phase time in the reflection or in the transmission mode. Thus in the present section we have chosen a simple and generalized geometry where we can analytically study the phase time in a reflection mode and in presence of Aharonov-Bohm flux. We show that this phase time in the opaque barrier regime becomes independent of the length of the circumference of the ring and the magnitude of the AB-flux. We have also studied this effect by including an additional potential well between two barriers in the circular ring (Fig. 9 (b)). Interestingly, the saturated reflection phase

time becomes independent of the length of the potential well (in the large length limit) for energy away from resonances. Inside the potential well the electron travels with a real velocity. Increasing or decreasing the free path (length of the well) does not alter the saturated reflection phase time through the system. It seems as if for the electronic wave the free space collapses. This result is regarded as a “space collapse” or “space destroyer”<sup>31</sup>.

### 3.1. Theoretical Treatment

We use the same quantum wave guide theory<sup>37,35</sup> as discussed in the earlier section. To set the equations in most general context we consider Fig. 9(b) in presence of flux  $\phi$ . The wave functions in different regions are

$$\psi_0(x_0) = e^{ikx_0} + r e^{-ikx_0} \quad (\text{in region I}) \quad (10)$$

$$\psi_1(x_1) = A_1 e^{-\kappa_1 x_1} + B_1 e^{\kappa_1 x_1} \quad (\text{in region II}) \quad (11)$$

$$\psi_w(x_w) = C e^{ikx_w} + D e^{-ikx_w} \quad (\text{in region III}) \quad (12)$$

$$\psi_2(x_2) = A_2 e^{-\kappa_2 x_2} + B_2 e^{\kappa_2 x_2} \quad (\text{in region IV}) \quad (13)$$

with  $k$  being the wave-vector of electrons in the lead and in the intermediate free space between two barriers inside the ring.  $\kappa_1 = \sqrt{2m(V_1 - E)/\hbar^2}$  and  $\kappa_2 = \sqrt{2m(V_2 - E)/\hbar^2}$  are the imaginary wave-vectors respectively for tunneling electrons in the barriers of strength  $V_1$  and  $V_2$  inside the ring. The origin of the co-ordinates of  $x_0$  and  $x_1$  is assumed to be at  $J_1$  and that for  $x_w$  and  $x_2$  at  $P_1$  and  $P_2$  respectively. At  $P_1$ ,  $x_1 = lb_1$ , at  $P_2$ ,  $x_w = w$  and at  $J_1$ ,  $x_2 = lb_2$ , where  $lb_1$  and  $lb_2$  are the length of the two barriers and  $w$  is the length of the well inside the ring. Total circumference of the ring is  $L = lb_1 + lb_2 + w$ .

In presence of the AB-flux, following the same method described above, the boundary conditions for the current system (shown in Fig. 9(b)) are

$$1 + r - A_1 - B_1 \exp(-i\alpha_1) = 0, \quad (14)$$

$$A_2 \exp(-\kappa_2 lb_2) \exp(i\alpha_2) + B_2 \exp(\kappa_2 lb_2) - 1 - r = 0, \quad (15)$$

$$ik(1 - r) + \kappa_1(A_1 - B_1 \exp(-i\alpha_1)) - \kappa_2 A_2 \exp(-\kappa_2 lb_2) \exp(i\alpha_2) - \kappa_2 B_2 \exp(\kappa_2 lb_2) = 0, \quad (16)$$

$$A_1 \exp(-\kappa_1 lb_1) \exp[i\alpha_1] + B_1 \exp(\kappa_1 lb_1) - C - D \exp(-i\alpha_w) = 0, \quad (17)$$

$$\kappa_1 A_1 \exp(-\kappa_1 lb_1) \exp(i\alpha_1) - \kappa_1 B_1 \exp(\kappa_1 lb_1) + ikC - ikD \exp(-i\alpha_w) = 0, \quad (18)$$

$$C \exp(ikw) \exp(i\alpha_w) + D \exp(-ikw) - A_2 - B_2 \exp(-i\alpha_2) = 0, \quad (19)$$

$$ikC \exp(ikw) - ikD \exp(-ikw) \exp(-i\alpha_w) + \kappa_2 A_2 - \kappa_2 B_2 \exp(-i\alpha_2) = 0, \quad (20)$$

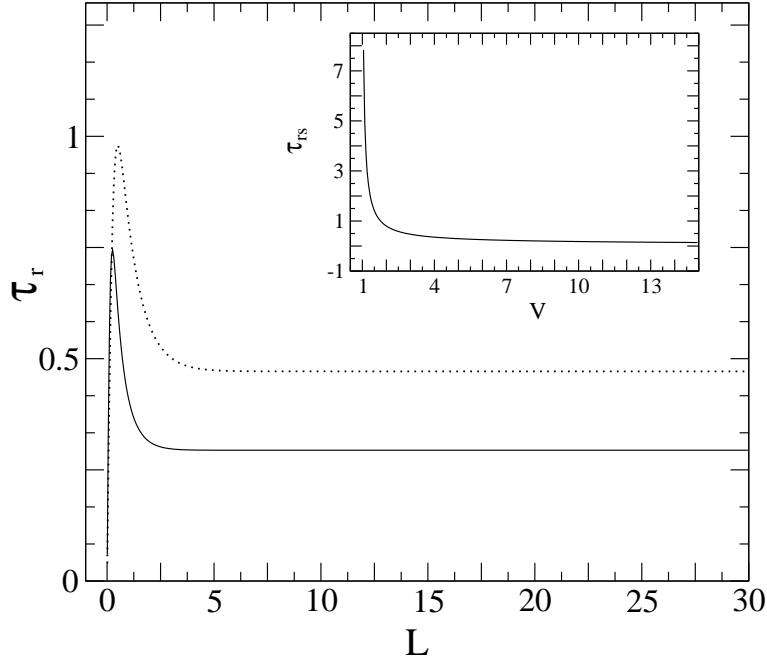


Fig. 10. In absence of magnetic flux (*i.e.*  $\phi=0$ ), for a ring with a barrier of strength  $V$  throughout its circumference, the reflection phase time  $\tau_r$  is plotted as a function of ring's circumference  $L$ . The solid, and dotted curves are for  $V = 5, 3$  respectively. Incident energy is set to be  $E = 1$ . In the inset the saturated value of phase time  $\tau_{r,s}$  is plotted as a function of the barrier's strength for same  $E$ .

where  $i\alpha_1, i(\alpha_1 + \alpha_w)$  are the phases picked up respectively at  $P_1$  and  $P_2$  by the electron traveling clockwise from  $J_1$  and  $i(\alpha_1 + \alpha_w + \alpha_2)$  is the phase picked up by the same electron at  $J_1$  after traversing once along the ring. The total phase around the ring becomes  $\alpha_1 + \alpha_w + \alpha_2 = 2\pi\phi/\phi_0$ .

To obtain an analytical expression for the reflection amplitude for a ring system as shown in Fig. 9(a) we solve Eqs. (14)- (20) using  $C = 0, D = 0, A_2 = A_1, B_2 = B_1, \kappa_2 = \kappa_1$  in the wave functions (12) and (13) and  $x_1 = L$  at  $J_1$  after a complete traversal along the circumference. The reflection amplitude is

$$r = \frac{-\kappa_1 (2 \cos(\alpha) - \exp(kL)) + i \frac{k}{2} \exp(kL)}{\kappa_1 (2 \cos(\alpha) - \exp(kL)) + i \frac{k}{2} \exp(kL)}, \quad (21)$$

where  $\alpha = 2\pi\phi/\phi_0$ . After knowing  $r$ , the 'reflection phase time'  $\tau_r$  can be calculated from the energy derivative of its phase<sup>5,14</sup> as

$$\tau_r = \frac{\partial \text{Arg}[r]}{\partial E}. \quad (22)$$



### 3.2. Results and Discussions

We now proceed to analyze the behavior of  $\tau_r$  as a function of various physical parameters for these ring systems. In the similar fashion, described above, here also we express all the physical quantities in dimensionless units. Thus the reflection phase time  $\tau_r$  is expressed in units of inverse of incident energy  $E$  ( $\tau_r \equiv E \tau_r$ ). After straight forward algebra in the large length ( $L$ ) limit and in absence of magnetic flux, we obtain an analytical expression for the saturated reflection phase time (using Eq. (21) in Eq. (22)), which is given by,

$$\tau_{r,s} = \frac{\frac{1}{k\kappa} + \frac{k}{\kappa^3}}{\left(2 + \frac{k^2}{2\kappa^2}\right)}, \quad (23)$$

with  $\kappa$  being the imaginary wave vector of the electron inside the barrier of strength  $V$  and length  $lb$  ( $= L$ ).

First we take up a ring system with a single barrier along the circumference of the ring as shown in Fig. 9(a). For a tunneling particle having energy less than the barrier strength we find out the reflection phase time  $\tau_r$  as a function of barrier length  $L$  which in turn is the circumference of the ring. We see (Fig. 10) that in absence of magnetic flux,  $\tau_r$  evolves as a function of  $L$  and asymptotically saturates to a value  $\tau_{r,s}$  which is independent of  $L$  thus confirming the ‘Hartman effect’. From Fig. 10 it is clear that the saturation value increases with the decreasing barrier-strength. In the inset of Fig. 10, we have plotted  $\tau_{r,s}$  as a function of barrier-strength. From this we can see that for electrons with incident energy close to the barrier-strength the value of  $\tau_{r,s}$  is quite large.

To see the effect of magnetic flux on ‘Hartman effect’, we consider the same system but in presence of AB-flux. We study the reflection phase time as a function of AB-flux for different values of the length  $L$  of the ring’s circumference. We have chosen the lengths such that in the absence of the ‘AB-flux’, for a given system (*i.e.*, for known  $E$  and  $V$ ) the reflection phase time  $\tau_r$  gets saturated for these lengths. From Fig. 11 we see that  $\tau_r$  as a function of  $\phi$  shows AB-oscillations with an average value which is the saturation value  $\tau_{r,s}$  for the same system in absence of AB-flux. Further we observe that (Fig. 11)  $\tau_r$  is flux periodic with periodicity  $\phi_0$ . This is consistent with the fact that all the physical properties in presence of AB-flux across the ring must be periodic function of the flux with a period  $\phi_0$ <sup>17,32,43</sup>. However, we see that as we increase  $L$  the magnitude of AB-oscillation in  $\tau_r$  decreases. Consequently in the large length limit the visibility of oscillations vanishes. This clearly establishes ‘Hartman effect’ even in presence of AB-flux. The constant value of  $\tau_r$  thus obtained in the presence of flux is identical to  $\tau_{r,s}$  (0.294115) in the absence of flux (see Fig. 11) in the large length regime and its magnitude is given by Eq. (23). This result clearly indicates that the reflection phase time in the presence of opaque barrier becomes not only independent of the length of the circumference but also is independent of the AB-flux thereby observing the ‘Hartman effect’ even in the presence of AB-flux. Since the magnetic field tunes the boundary conditions and in

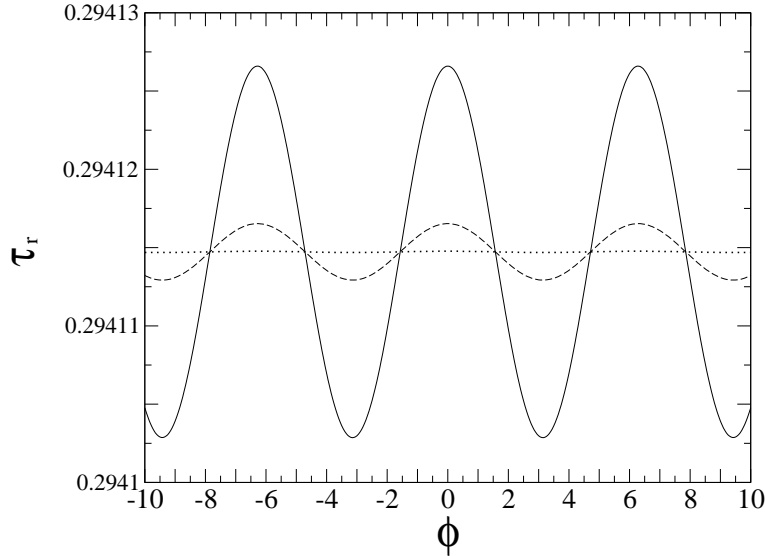


Fig. 11. For a ring with a barrier of strength  $V$  lies throughout its circumference, the saturated phase time  $\tau_{r,s}$  is plotted as a function of magnetic flux  $\phi$ . The solid, dashed and dotted curves are for  $L = 6, 7, 9$  respectively. Other system parameters are  $V = 5, E = 1$ .

the large length limit the evanescent states become insensitive to the boundaries (as they decay out before reaching the boundary) the Hartman effect follows.

Now we consider the ring system with the ring having two successive barriers separated by an intermediate free space (we shall call it ‘quantum well’ in what follows) as shown in Fig. 9(b). In the absence of magnetic flux, we see the effect of ‘quantum well’ on the reflection phase time  $\tau_r$ . In Fig. 12  $\tau_r$  is plotted as a function of one of the barrier length (say  $lb_1$ ) while other barrier length is kept fixed ( $lb_2 = 5$ ) and for few different values of length of the well. Here, the fixed value of  $lb_2$  is chosen in such a way that in absence of the well region the reflection phase time reaches saturation at this length. From Fig. 12 we see that for all parameter values of well length, the saturation value of reflection phase time  $\tau_{r,s}$  is same and it is equal to what we obtained in absence of the well in the ring system. Thus the saturated phase time becomes independent of the length of the well (in the long length limit) for the energy away from the resonances. This is as if the effective velocity of the electron in the well becomes infinite or equivalently length of the well does not count (space collapse or space destroyer) while traversing the ring.

Next we consider a similar system as that shown in Fig. 9(b). Here we see the effect of resonances present in the ring system with the well, on the saturated reflection phase time  $\tau_{r,s}$ . For the system described above with two identical barriers

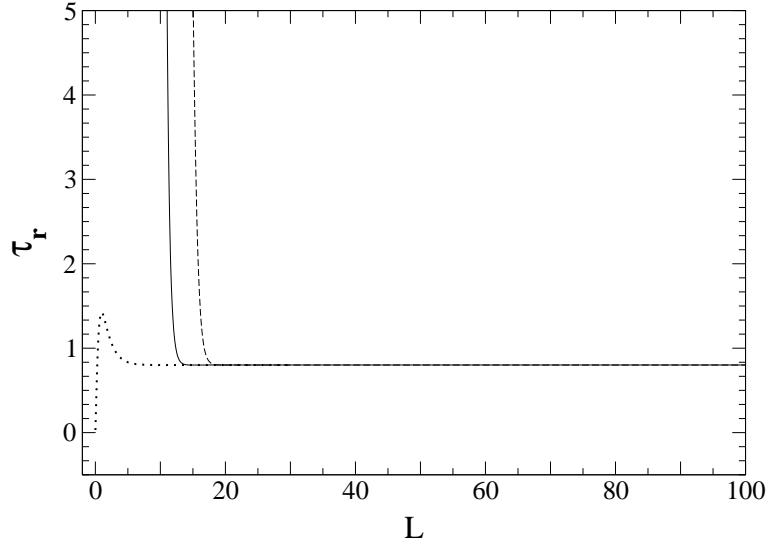


Fig. 12. In absence of magnetic flux (*i.e.*  $\phi = 0$ ), for a ring with two barriers of strength  $V_1$  and  $V_2$  separated by an intermediate well region, the reflection phase time  $\tau_r$  is plotted as a function of ring's circumference  $L$  for different length  $w$  of the well. The dotted, solid and dashed curves are for  $w = 0, 5, 10$  respectively. Other system parameters are  $lb_2 = 5$ ,  $V_1 = V_2 = 2$  and  $E = 1$ .

of strength  $V_1 = V_2 = 2$  and length  $lb_1 = lb_2 = 5$  separated by an intermediate free space of length  $w$  we study the phase time  $\tau_r$  as a function of  $w$  in absence of the magnetic flux ( $\phi = 0$ ). In Fig. 13(a) we have plotted  $\tau_{r,s}$ , for the electrons with an incident energy  $E = 1.5$ . It should be noted that as we increase the length of the well the incident energy  $E$  coincides with resonances (or resonant states) in the well (which arise due to constructive interference due to multiple scatterings inside the well). For these values of  $w$  we observe sharp rise in the saturated delay time and its magnitude depends on the length of the well. We see that the resonances which have Lorentzian shape become broader as the length of the free region  $w$  becomes large. It is worthwhile to mention that away from the resonance the value of  $\tau_{r,s}$  is independent of the length of the well (see Fig.12) and depends only on the barrier strength. The resonance being dependent on the incident energy of the electrons we follow a particular resonance peak (say, the first peak) in  $\tau_{r,s}$  for different  $E$ . In Fig. 13(b), the first peak values are plotted as a function of  $w$  for seven different incident energies in the sub-barrier tunneling regime. We see that as we increase the incident energy the resonances shift towards lower  $w$  value and also the peak-value decreases as expected. The above result clearly indicate that at and around the resonance the saturated value depends on the length of the free space, however, away from the resonance the saturated delay time is independent of the length of the free space( space collapse or space destroyer as discussed earlier).

20 Swarnali Bandopadhyay, A. M. Jayannavar

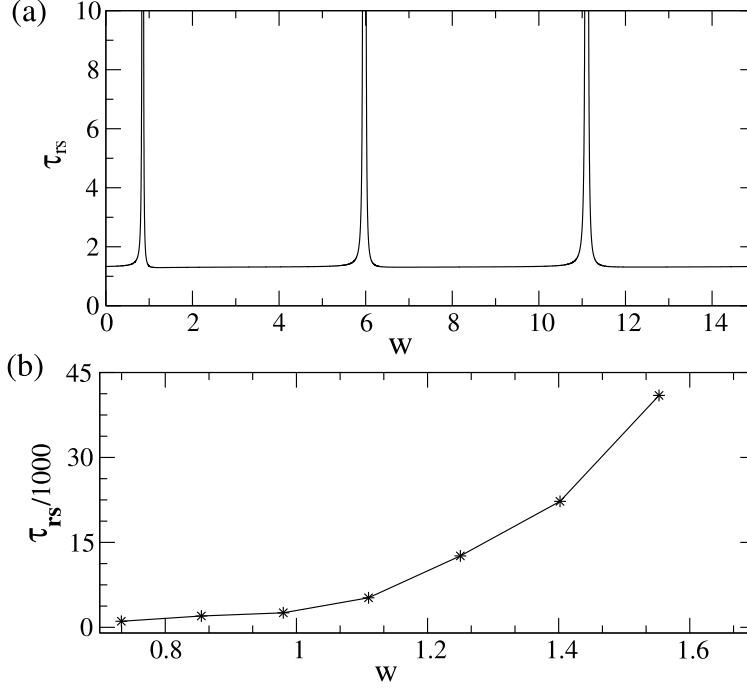


Fig. 13. (a) In absence of magnetic flux (*i.e.*  $\phi = 0$ ), for a ring with two identical barriers ( $V_1 = V_2 = 2$ ,  $lb_1 = lb_2 = 5$ ) separated by an intermediate well region of length  $w$ , the phase time  $\tau_r$  is plotted as a function of  $w$  at  $E = 1.5$ . (b) With change in incident energy the position of resonance peaks shift. We follow the first resonance peak and plot resonant phase time  $\tau_r^*$  as a function of  $w$  as we vary incident energy. From left to right the points correspond to energies  $E = 1.6, 1.5, 1.4, 1.3, 1.2, 1.1, 1.01$  respectively.

Instead of a real barrier we now consider a complex potential (or absorption)  $V = V_{re} - iV_{im}$  in Fig. 9(a). Here,  $V_{re}$  represents the real strength of the barrier whereas  $V_{im}$  is the imaginary strength. In presence of the imaginary part in the potential our ring system can absorb particles in it. Earlier Raciti *et. al.*, have shown<sup>44</sup> that the phase time in transmission mode for an absorptive one-dimensional rectangular barrier does not show the saturation in opaque barrier limit, instead, it is linearly proportional to the length of the barrier. Thus they conclude that in presence of strong absorption the tunneling time does not show the Hartman effect. We have separately studied the phase time in both transmission and reflection modes of the one-dimensional complex barrier. We have found that in presence of non-negligible absorption in the large length limit of the barrier though the transmission phase time does not saturate the reflection phase time shows Hartman effect. It would be worth to mention here that the saturated reflection phase time of

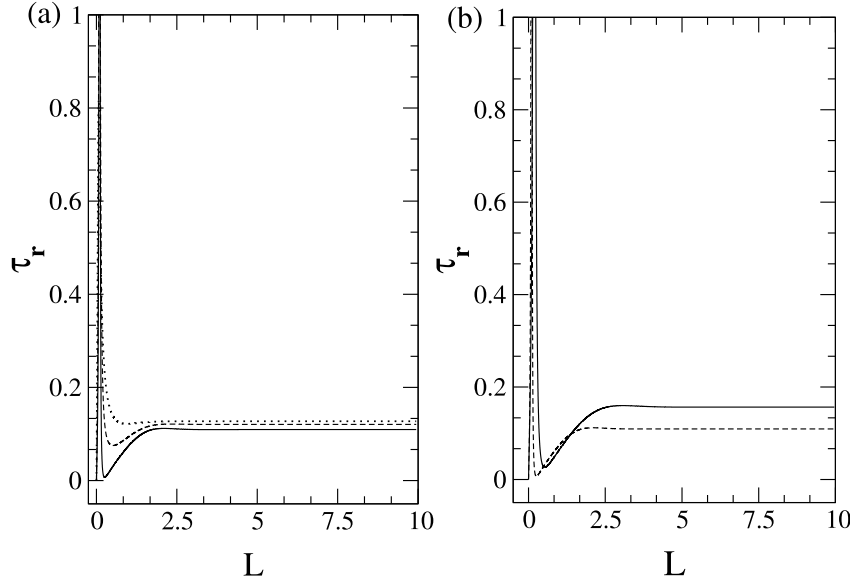


Fig. 14. In presence of a complex barrier covering the ring's circumference the phase time  $\tau_r$  in reflection mode is plotted as a function of ring's circumference. In (a) the three different curves are for three different strength of the real part of the potential while the imaginary part is fixed at  $V_{im} = 10$ . The solid, dashed and dotted curves are for  $V_{re} = 2, 4$  and  $10$  respectively. In (b) the  $\tau_r$  is plotted for two different values of the imaginary part of the potential keeping the strength fixed at  $V_{re} = 2$ . The solid and dashed curves are for  $V_{im} = 5$  and  $10$  respectively. Incident energy is set to be  $E = 1$ .

1D complex barrier is same as that for an one-dimensional complex step potential. Now we study the phase time in reflection mode (Fig. 9(a)) in the presence of a complex potential. We vary the barrier length (ring circumference) for different values of  $V_{re}$  and  $V_{im}$ . From Fig. 14, we see that even in presence of complex potential Hartman effect survives for our ring system. In Fig. 14(a), keeping the imaginary part of the potential fixed we vary the strength of the barrier. We see that the saturated phase time as well as the nature of evolution of the  $\tau_r$  as a function of  $L$  depend on  $V_{re}$ . From Fig. 14(b), we see that the saturated reflection phase time changes with  $V_{im}$  as well.

Finally we consider a quantum ring connected with two identical leads as shown in Fig. 15. Each of the two arms (say upper and lower arm) of the ring are covered entirely by a barrier. We study the transmission phase time in the absence

22 Swarnali Bandopadhyay, A. M. Jayannavar

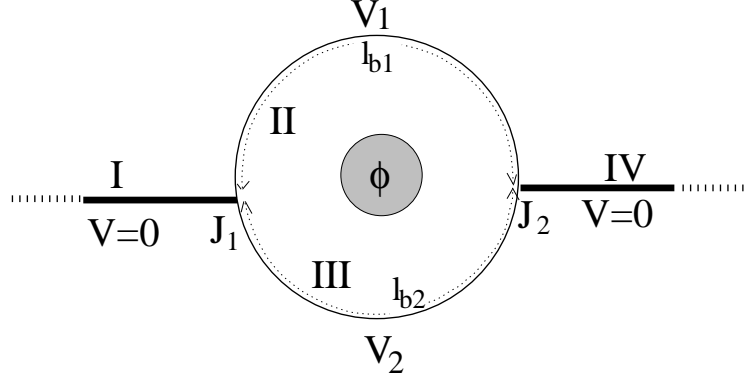


Fig. 15. Schematic diagram of a ring connected to two leads at the junctions  $J_1$  and  $J_2$  in the presence of an Aharonov-Bohm flux,  $\phi$ . The upper arm of the ring is covered by a barrier of strength  $V_1$  and length  $lb_1$ . Similarly, the lower arm is covered by a barrier of strength  $V_2$  and length  $lb_2$ . The circumference of the ring is  $L = lb_1 + lb_2$ .

of magnetic flux by varying different system parameters. Here also the phase time evolves with increasing length of the barriers and for larger length the phase time gets saturated. The saturation value does not depend on the ratio of the length of the two arms of the ring. However, this value depends on the incident energy of the particles. In Fig. 16 we have plotted the saturated transmission phase time  $\tau_{ts}$  as a function of incident energy  $E/V$  for  $\phi = 0$ . The circumference of the ring is taken as  $L = 30$  with equal upper and lower arm lengths. Plots with different arm length ratios ( $lb_1 : lb_2$ ) with different  $\phi$  in the asymptotic limit were found to overlap with the above curve in the entire energy regime. Analytically, in the large  $L$  ( $> 1/\kappa$ ) limit, the transmission phase time  $\tau_t$  becomes independent of  $L$  and the magnetic flux (in accordance with Hartman effect) and is given by

$$\tau_{ts} = \frac{4\kappa^3 + 5k^2\kappa + (k^4/\kappa)}{2k((2\kappa^2 - (k^2/2))^2 + 4k^2\kappa^2)}. \quad (24)$$

#### 4. Conclusions

We have verified the Hartman effect in quantum network consisting of an one dimensional arm having two side branches. These side branches may or may not have barriers. In presence of a barrier, the ‘phase time’ for transmission through a side branch shows the ‘Hartman effect’. Due to quantum nonlocality the ‘phase time’ and its saturated value at any side branch feel the presence of barriers in other branches. Thus one can tune the saturation value of ‘phase time’ and consequently the superluminal speed in one branch by changing barrier parameters in any other branch which is spatially separated from the former. Moreover, Hartman effect with negative saturation times (time advancement) has been observed for some parameter values. The phase times are also sensitive to the junction  $S$ -matrix elements used

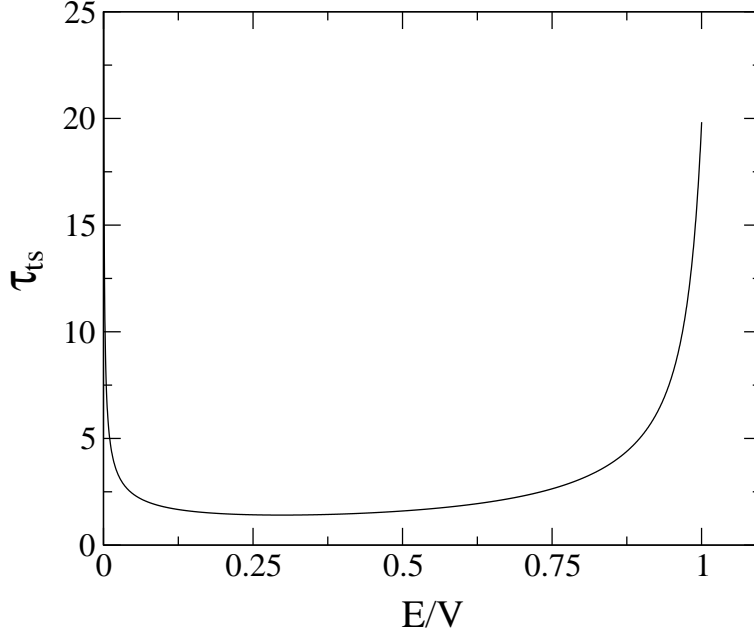


Fig. 16. In absence of magnetic flux (*i.e.*  $\phi=0$ ), for a ring shown in Fig. 15 the saturated transmission phase time  $\tau_{ts}$  is plotted as a function of incident energy  $E/V$ . The length of the identical barriers ( $V_1 = V_2$ ,  $l_{b1} = l_{b2}$ ) in the upper and lower arms of the ring are  $L/2 = 15$ .

for a given problem. Depending on  $w_n$  there may be one or several bound states located between the barriers in different branched arms and as a consequence saturated delay time can be varied from the negative (ultra Hartman effect) to positive and vice-versa. We have verified this by looking at the transmission coefficient in the second arm  $S_2$  which exhibits clear resonances as a function of  $w_2$ . Moreover the reported effects are amenable to experimental verifications in the electromagnetic wave-guide networks.

We have further extended our studies on Hartman effect in quantum ring geometry in the presence of AB flux. We have studied the quantum reflection phase time for a ring connected with a single lead. Our study show that the phase time for a given incident energy becomes independent of the barrier thickness as well as the magnitude of the flux in the limit of opaque barrier. In the absence of AB-flux we have obtained analytical expressions for the saturated reflection and transmission phase times for the ring geometries. In addition, introducing a potential well between two successive opaque barriers covering the entire circumference of the ring, we have found that the saturated reflection phase time becomes independent of the length of the well for energies away from the resonances. This implies, as if, the effective velocity of the electron within the well becomes infinite or equivalently the length of the well does not count (space collapse or space destroyer). Earlier

24 *Swarnali Bandopadhyay, A. M. Jayannavar*

studies reveal that the Hartman effect disappears in presence of complex barrier in a transmission mode. We have shown that the Hartman effect survives in the reflection mode.

## 5. Acknowledgments

One of the authors (SB) thanks Doron Cohen and Debasish Chaudhuri for useful discussions. SB also thanks SNBNCBS, Kolkata and IOP, Bhubaneswar where a large part of the present work was carried out.

1. R. Tsu and L. Esaki, *Appl. Phys. Lett.* **22**, 562 (1973).
2. G. Binning and H. Rohrer, *IBM J. Res. Dev.* **30**, 355 (1986).
3. L. A. MacColl, *Phys. Rev.* **40**, 621 (1932).
4. R. Landauer and T. Martin, *Rev. Mod. Phys.* **66**, 217 (1994).
5. E. H. Hauge and J. A. Støvneng, *Rev. Mod. Phys.* **61** 917 (1989).
6. S. Anantha Ramakrishna and N. Kumar, *Europhys. Lett.*, 60 491 (2002); Colin Benjamin and A. M. Jayannavar, *Solid State Commun.*, 121 591 (2002).
7. A. M. Steinberg, P. G. Kwiat, and R. Y. Chiao, *Phys. Rev. Lett.* **71** 708 1993; R. Y. Chiao, P. G. Kwiat, and A. M. Steinberg, *Scientific American*, p. 38-46, August 1993.
8. A. Enders and G. Nimtz, *J. Phys. I* **2** 1693 (1992); **3** (1993) 1089; A. Enders and G. Nimtz, *Phys. Rev. E*, **48**, 632 (1993); G. Nimtz, A. Enders and H. Spieker, *ibid* **4** (1994) 565.
9. S. Collins, D. Lowe and J. R. Barker, *J. Phys. C* **20**, 6213 (1987); R. S. Dumont and T. L. Marchioro II, *Phys. Rev. A* **47**, 85 (1993).
10. P. Guerent, E. Marclay, and H. Meier, *Solid State Commun.* **68**, 977 (1988); Ch. Spielmann, R. Szipocs, A. Sting, and F. Krausz, *Phys. Rev. Lett.* **73**, 2308 (1994); Th. Hills et al., *Phys. Rev. A* **58**, 4784 (1998).
11. F. T. Smith *Phys. Rev.* **113**, 349 (1960).
12. M. Büttiker and R. Landauer, *Phys. Rev. Lett.* **49**, 1739 (1982).
13. M. Büttiker, *Phys. Rev. B* **27**, 6178 (1983).
14. E. P. Wigner, *Phys. Rev.* **98** 145 (1955).
15. T. E. Hartman, *J. Appl. Phys.* **33** (1962) 3427.
16. E. H. Hauge, J. P. Falck, and T. A. Fjeldly, *Phys. Rev. B* **36**, 4203 (1987).
17. M. Büttiker, *J. Phys. Condensed Matter*, **5** (1993) 9361; M. Büttiker, H. Thomas and A. Prêtre, *Phys. Lett. A* **180** (1993) 364.
18. M. Büttiker, *Pramana Journal of Physics*, **58**, 241 (2002).
19. Y. Avishai and Y. B. Band, *Phys. Rev. B* **32**, 2674 (1985); Roger Dashen, Shang-keng Ma, and Herbert J. Bernstein, *Phys. Rev.* **187**, 345(1969).
20. P. Singha Deo, Swarnali Bandopadhyay and Sourin Das, *Int. J. Mod. Phys. B*, **16**, 2247 (2002).
21. S. Bandopadhyay, P. Singha Deo, *Phys. Rev. B* **68**, 113301 (2003).
22. A. M. Jayannavar, G. V. Vijaygobindan and N. Kumar, *Z. Phys. B* **75** (1989) 77; Sandeep K. Joshi, A. Kar Gupta and A. M. Jayannavar, *Phys. Rev.* **B58** (1998) 1092; Sandeep K. Joshi and A. M. Jayannavar, *Solid State Commun.* **106** (1998) 363; *ibid* **111** (1999) 547; For a review see Yan Fyodorov and H. Sommers, *J. Math. Phys.* **38** (1997) 1918.
23. V. S. Olkhovsky and E. Recami, *Physics Reports* **214** 339 (1992).
24. J. R. Fletcher, *J. Phys. C* **18**, L55 (1985).



25. On Universal Properties of Tunnelling, G. Nimtz et al., APEIRON **7**, Nr. 1-2, January - April, 2000.
26. A. Haibel and G. Nimtz, Ann. Phys. (Leipzig) **10**, ed. 8, 707-712 (2001).
27. H. G. Winful, Phys. Rev. Lett. **91** (2003) 260401; H. G. Winful, Phys. Rev. **E68** (2003) 016615; H. G. Winful, Opt. Express **10** (2002) 1491.
28. Swarnali Bandopadhyay, Raishma Krishnan and A. M. Jayannavar, Solid State Commun. **131**, 447 (2004).
29. Swarnali Bandopadhyay and A. M. Jayannavar, Phys. Lett. A, **335**, 266 (2005).
30. Swarnali Bandopadhyay and A. M. Jayannavar, Indian Journal of Physics **79**, 953 (2005).
31. V. S. Olkhovsky, E. Recami and G. Salesi, Europhys. Lett. **57** 879 (2002).
32. S. Washburn and R. A. Webb, Adv. Phys. **35**, 375 (1986).
33. Y. Gefen, Y. Imry and M. Ya Azbel, Phys. Rev. Lett. **52** (1984) 129.
34. B. C. Satishkumar, P. John Thomas, A. Govindaraj, and C. N. R. Rao, *Applied Physics Letters* **77(16)** 2530 (2000).
35. A. M. Jayannavar and P. Singha Deo, Mod. Phys. Lett. B **8** (1994) 301-310.
36. B. C. Gupta, P. Singha Deo and A. M. Jayannavar, Int. J. Mod. Phys. B **10** 3595 (1996); Colin Benjamin and A. M. Jayannavar, Phys. Rev. B **68** 085325 (2003).
37. J. B. Xia, Phys. Rev. **B45** (1992) 3593.
38. P. S. Deo and A. M. Jayannavar, Phys. Rev. B, **50**, 11629 (1994).
39. S. Griffith, Trans. Faraday Soc. **49**, 650 (1953).
40. J. G. Muga, I. L. Egusquiza, J. A. Damborenea, and F. Delgado, Phys. Rev. A, **66**, 042115 (2002).
41. M. Büttiker, Phys. Rev. B **32**, 1846 (1985).
42. B. Shapiro, Phys. Rev. Lett. **50**, 747 (1983).
43. S. Datta, *Electronic Transport in Mesoscopic Systems*, Cambridge University Press, Cambridge, UK, (1997).
44. Fabio Raciti and Giovanni Salesi, J. de Phys.(France) **I4**, 1783 (1994).